

Article

Electrochemical Detection of *ompA* Gene of *C. sakazakii* Based on Glucose-Oxidase-Mimicking Nanotags of Gold-Nanoparticles-Doped Copper Metal-organic Frameworks

Hongyan Zhang ¹, Guiqing Xu ¹, Yuming Chen ², Xu Li ¹, Shaopeng Wang ¹, Feihao Jiang ², Pengyang Zhan ², Chuanfu Lu ², Xiaodong Cao ¹ , Yongkang Ye ^{1,*}  and Yunlai Tao ³

¹ School of Food Science and Biological Engineering, Hefei University of Technology, Hefei 230009, China; xiaodongcao@hfut.edu.cn (X.C.)

² Department of Food Science, Xuancheng Campus, Hefei University of Technology, Xuancheng 242000, China

³ Anhui Institute of Food and Drug Inspection, Hefei 230051, China; tyl3333@sohu.com

* Correspondence: yongkang.ye@hfut.edu.cn

Abstract: The present work developed an electrochemical genosensor for the detection of virulence outer membrane protein A (*ompA*, tDNA) gene of *Cronobacter sakazakii* (*C. sakazakii*) by exploiting the excellent glucose-oxidase-mimicking activity of copper Metal-organic frameworks (Cu-MOF) doped with gold nanoparticle (AuNPs). The signal nanotags of signal probes (sDNA) that biofunctionalized AuNPs@Cu-MOF (sDNA-AuNPs@Cu-MOF) were designed using an Au-S bond. The biosensor was prepared by immobilization capture probes (cDNA) onto an electrodeposited AuNPs-modified glassy carbon electrode (GCE). AuNPs@Cu-MOF was introduced onto the surface of the GCE via a hybridization reaction between cDNA and tDNA, as well as tDNA and sDNA. Due to the enhanced oxidase-mimicking activity of AuNPs@Cu-MOF to glucose, the biosensor gave a linear range of 1.0×10^{-15} to 1.0×10^{-9} mol L⁻¹ tDNA with a detection limit (LOD) of 0.42 fmol L⁻¹ under optimized conditions using differential pulse voltammetry measurement (DPV). It can be applied in the direct detection of *ompA* gene segments in total DNA extracts from *C. sakazakii* with a broad linear range of $5.4\text{--}5.4 \times 10^5$ CFU mL⁻¹ and a LOD of 0.35 CFU mL⁻¹. The biosensor showed good selectivity, fabricating reproducibility and storage stability, and can be used for the detection of *ompA* gene segments in real samples with recovery between 87.5% and 107.3%.

Keywords: electrochemical biosensor; *C. sakazakii*; gold-nanoparticle-doped copper Metal-organic frameworks; *ompA* gene; glucose-oxidase-mimicking activity



Citation: Zhang, H.; Xu, G.; Chen, Y.; Li, X.; Wang, S.; Jiang, F.; Zhan, P.; Lu, C.; Cao, X.; Ye, Y.; et al. Electrochemical Detection of *ompA* Gene of *C. sakazakii* Based on Glucose-Oxidase-Mimicking Nanotags of Gold-Nanoparticles-Doped Copper Metal-organic Frameworks. *Sensors* **2023**, *23*, 4396. <https://doi.org/10.3390/s23094396>

Academic Editors: Simone Morais, Álvaro Miguel Carneiro Torrinha and Iria Bravo

Received: 2 April 2023
Revised: 27 April 2023
Accepted: 28 April 2023
Published: 29 April 2023



Copyright: © 2023 by the authors. Licensee MDPI, Basel, Switzerland. This article is an open access article distributed under the terms and conditions of the Creative Commons Attribution (CC BY) license (<https://creativecommons.org/licenses/by/4.0/>).

1. Introduction

Cronobacter sakazakii (*C. sakazakii*), widely found in various kinds of foods, is one of the most dangerous foodborne pathogens for infants and young children [1,2]. It is reported that the mortality rate for the *C. sakazakii*-infected patients is about 40–80% and the pollution source is unclear [3,4]. What is more serious is that the pathogenic mechanism has not been clarified yet. Therefore, rapid prevention, detection, and screening of *C. sakazakii* are particularly important to ensure food safety and quality.

The bacterial culture method for *C. sakazakii* is a traditional method that takes 5 to 7 days to obtain results and cannot meet the needs for rapid detection and screening of bacteria. Some other methods that are classified into protein-based biosensing method [5–7] and DNA-based biosensing method [8–16] have been promoted and applied in the detection of *C. sakazakii*. Protein-based immunoassays, such as enzyme-linked immunosorbent assays (ELISAs) [5] and lateral flow immunoassays [6], are based on antibody-antigen interactions, which require a certain concentration of targets in samples, and sometimes cannot be applied in the detection at an early infection stage. DNA-based methods including polymerase chain reaction (PCR)-based biosensing methods [8,9], fluorescence biosensing

methods [10,11], colorimetric biosensing methods [12,13], and electrochemical biosensing methods [14–16] have been intensively promoted and investigated for the detection of *C. sakazakii*. Due to the properties of low cost, ease of fabrication, time-saving, and ease of operation, several kinds of electrochemical biosensors, including amperometric biosensors [14,16] and voltametric biosensors [15], have been fabricated for *C. sakazakii* detection. To enhance the sensitivity of *C. sakazakii* detection, nanomaterials and signal amplification strategies have been used in biosensor construction and *C. sakazakii* detection. For instance, Peng et al. [15] constructed a sensitive electrochemical aptasensor using the nanomaterial of methylene blue (MB)-anchored graphene oxide (GO). By using the large surface area and abundant recognition sites of GO, the electrochemical oxidation signal MB was significantly enhanced. The fabricated biosensor showed a low detection limit of 7 CFU mL^{-1} ($S/N = 3$).

Metal-organic frameworks (MOF) are a type of inorganic-organic hybrid nanomaterial, in which the metal ions act as the connectors and the organic ligands as the linkers [17]. It has been widely used in energy storage [18–20], gas storage and separation [21], drug delivery [22], chemical sensors [23], and biosensors [24] due to the properties of large surface area, tunable structure, good catalytic activity, and biocompatibility. Cu-MOF as a member of the MOF family has been commonly used in fabricating chemical sensors [25,26] and biosensors [27,28] by utilizing its good conductivity, large surface area, excellent catalytic ability, and ease of surface modification. Research shows that Cu-based MOF have excellent mimic oxidase activities to various molecules, such as H_2O_2 [25,29,30], ascorbate [26], and glucose [30–33].

Gold nanoparticles (AuNPs) and AuNP-based nanomaterials have been proven to be excellent electrocatalysts to glucose [34,35]. In the present work, we constructed a DNA biosensor for the virulence outer membrane protein A (*ompA*) gene of *C. sakazakii* based on glucose-oxidase-mimicking AuNPs-doped Cu-MOF (AuNPs@Cu-MOF). As shown in Figure 1, Cu-MOF was prepared using 2-aminoterephthalic acid ($\text{NH}_2\text{-BDC}$) as a ligand, Cu(II) as a metal center, and triethylamine as a structure regulator. The prepared Cu-MOF was then used as carriers for doping AuNPs to synthesize AuNPs@Cu-MOF. Then signal probe DNA (sDNA) was immobilized on AuNPs@Cu-MOF via Au-S bond, forming signal nanotags of sDNA-AuNPs@Cu-MOF. The biosensor was constructed on a glassy carbon electrode modified in sequence with electrodeposited AuNPs, capture probe DNA (cDNA) for target *ompA* gene (tDNA), and BSA. Subsequently, tDNA was hybridized with cDNA and sDNA-AuNPs@Cu-MOF, bringing AuNPs@Cu-MOF to the surface of the modified electrode. Owing to the excellent mimic oxidase activity of AuNPs@Cu-MOF to glucose, the biosensor exhibited good analytical performance to target the *ompA* gene and *C. sakazakii* with a detection limit of 0.42 fmol L^{-1} and 0.35 CFU mL^{-1} .

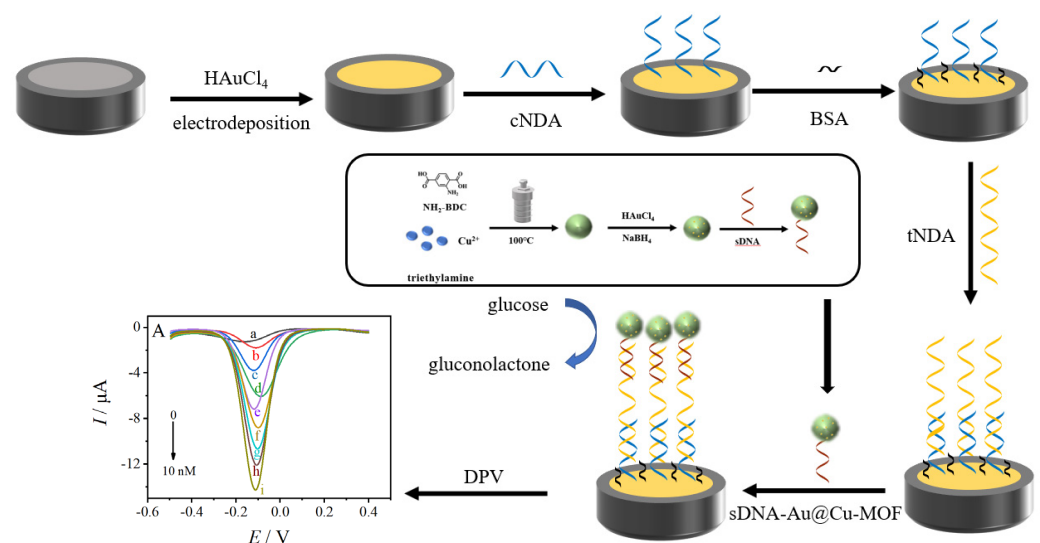


Figure 1. A schematic illustration of the fabrication of the biosensor.

2. Experimental Section

2.1. Materials

Polyvinylpyrrolidone K30 (PVP), N,N-dimethylformamide (DMF), ethanol, glucose, triethylamine, Tris-(2-carboxyethyl) phosphine (TCEP), 2-aminoterephthalic acid (NH₂-BDC, 99%), and bovine serum albumin (BSA, 98%) were purchased from Aladdin Industrial Co., Ltd. (Shanghai, China). Chloroauric acid (HAuCl₄), copper nitrate-trihydrate (Cu(NO₃)₂·3H₂O), and ethylenediaminetetraacetic acid disodium salt dihydrate (C₁₀H₁₄N₂Na₂O₈·2H₂O) were obtained from National Medicine Group Shanghai Chemical Reagent Co., Ltd. (Shanghai, China). TAE (50×) and Taq PCR Mix (2×) were purchased from Shanghai Sangon Biotechnology Co., Ltd. (Shanghai, China). All other chemicals were of analytical grade and used without further treatment. The buffers used in this work were as follows: (1) DNA stock buffer (pH 7.4): a mixture of 10 mmol L⁻¹ Tris-HCl and 1.0 mmol L⁻¹ EDTA; (2) DNA immobilization buffer (pH 7.4): a mixture of 10 mmol L⁻¹ Tris-HCl, 1.0 mmol L⁻¹ EDTA, 1.0 mmol L⁻¹ TCEP, 100 mmol L⁻¹ NaCl, and 1.0 mmol L⁻¹ MgCl₂; (3) DNA hybridization buffer (pH 7.4): 10 mmol L⁻¹ Tris-HCl, 1.0 mmol L⁻¹ EDTA, 100 mmol L⁻¹ NaCl, and 1.0 mmol L⁻¹ MgCl₂; (4) electrochemical detection buffer (pH 7.0): 0.1 mol L⁻¹ phosphate-buffered solution (PBS) containing 6.0 mmol L⁻¹ glucose. All the solutions were freshly prepared using ultrapure water (resistivity ≥ 18 MΩ cm).

All DNA sequences purchased from Shanghai Sangon Biotechnology Co., Ltd. (Shanghai, China) are listed in Table 1. Strains were provided by the Technology Center of Hefei Customs District. The total DNA of cultivated strains was extracted by using Bacterial Genomic DNA Rapid Extraction Kit (071011 M, 48 T) which was from Guangzhou Double Helix Gene Technology Co., Ltd. (Guangzhou, China).

Table 1. Nucleotide sequences used in the present work.

DNA Sample	Sequences
cDNA	5'-SH-AGC ATG CCG-3'
tDNA	5'-CGC TCG TCC GGA CAA CGG CAT GCT-3'
sDNA	5'-SH-TTG TCC GGA CGA GCG-3'
Mis-1	5'-CGC TCG TCC GGA CAA CGG CTT GCT-3'
Mis-2	5'-CGC TCG TGC GGA CAA CGG CTT GCT-3'
Mis-3	5'-CGC TCG TGC GGA CAA CCG CTT GCT-3'
NC	5'-ACT AGC CTT CCT TGG GAA GTA CTC-3'
Primer F	5'-CAT TGG TGA CGC GCA GAC T-3'
Primer R	5'-TGG ACG GGA TAC CTT TGG-3'

2.2. Apparatus

Scanning electron microscopy (SEM, Gemini 300, Zeiss, Jena, Germany) was carried out at an accelerating voltage of 3.0 kV, and X-ray photoelectron spectroscopy (XPS) measurements were conducted on an ESCALAB 250XI (Thermo Fisher Scientific, Waltham, MA, USA). The PCR reaction was conducted on TC-96/T/H PCR Amplifier (Hangzhou Bioer Technology Co., Ltd., Hangzhou, China). All the electrochemical measurements in terms of cyclic voltammetry (CV), electrochemical impedance spectroscopy (EIS), and differential pulse voltammetry (DPV) were performed on a CHI660D electrochemical workstation (Chenhua Instruments Inc., Shanghai, China) with a traditional three-electrode configuration. While performing measurements, a modified glassy carbon electrode (GCE), a platinum wire, and an Ag/AgCl (sat. KCl) electrode were used as the working, counter, and reference electrodes, respectively.

2.3. Synthesis of AuNPs@Cu-MOF

The Cu-MOF was prepared according to the literature [32,33] with some revisions. Typically, solution A was prepared by dissolving 0.2 g PVP in a mixture containing 4 mL DMF and 4 mL ethanol, and solution B was prepared by mixing 18.1 mg Cu(NO₃)₂·3H₂O and 5.4 mg NH₂-BDC in 4 mL DMF. Then, solution B was added into solution A, and

ultrasonicated for 5 min, followed by the addition of 2 μL triethylamine. The mixture was thoroughly mixed and then transferred into a Teflon-lined autoclave. The hydrothermal reaction was performed at 100 $^{\circ}\text{C}$ for 6 h. After cooling down to room temperature, the precipitate was collected, dissolved in 20 mL of DMF again, and reacted at 100 $^{\circ}\text{C}$ in the Teflon-lined autoclave for a further 8 h. Finally, the obtained Cu-MOF were centrifuged and freeze-dried for further use.

AuNPs@Cu-MOF was prepared by in situ reduction of AuCl_4^- on the surface of Cu-MOF. Briefly, Cu-MOF (10 mg) was first dispersed in 5 mL of deionized water. Then, 20 μL of 1% HAuCl_4 and 2 mL of 2 mmol L^{-1} NaBH_4 were added into the Cu-MOF dispersion with gentle shaking. The reaction was then performed at 4 $^{\circ}\text{C}$ for 1 h with continuous stirring. After centrifugation and washing several times, the obtained AuNPs@Cu-MOF was finally redispersed in a 2 mL DNA immobilization buffer.

2.4. Preparation of sDNA-Functionalized AuNPs@Cu-MOF Signal Probes

sDNA-functionalized AuNPs@Cu-MOF (sDNA-AuNPs@Cu-MOF) was prepared through the reaction between Au and $-\text{SH}$. A volume of 100 μL of 10 μM thiolated sDNA was added into the dispersion of AuNPs@Cu-MOF, followed by shaking for 12 h at 4 $^{\circ}\text{C}$. The obtained sDNA-AuNPs@Cu-MOF was centrifuged and washed several times and then dispersed in DNA storage buffer (2 mL) and stored at 4 $^{\circ}\text{C}$.

2.5. Fabrication of the ompA Biosensor

The *ompA* biosensor was fabricated on the GCE surface (Figure 1). Before modification, bare GCE was polished with 1.0, 0.3, and 0.05 μm $\alpha\text{-Al}_2\text{O}_3$ slurry, ultrasonicated in ethanol and water in sequence, and finally dried under nitrogen flow to obtain a clean, mirror-like surface. Firstly, the pretreated GCE was immersed in 0.1 mol L^{-1} KNO_3 (5 mL) solution containing 3.0 mmol L^{-1} HAuCl_4 . The electrode was then operated at a constant potential of -0.2 V for 70 s to obtain electrodeposited AuNPs-modified GCE (Au/GCE). Secondly, 10 μL of 1 $\mu\text{mol L}^{-1}$ cDNA was cast onto the Au/GCE and then capped with a centrifuge tube on top and kept at 4 $^{\circ}\text{C}$ for 12 h. Then, the electrode was rinsed with 0.1% SDS solution and Tris-HCl solution (10 mmol L^{-1} , pH = 7.4) to remove the unbound capture probe. The modified electrode was denoted as cDNA/Au/GCE. Finally, the *ompA* biosensor was accomplished by immersing cDNA/Au/GCE in 1% BSA for 30 min to eliminate nonspecific adsorption.

2.6. Preparation of DNA Samples and PCR of the ompA Gene Products

The preparation of DNA samples and PCR products of *ompA* gene segments was according to our previous work [14,36]. First, *C. sakazakii* solution with various concentrations was prepared according to previous work with slight modification [14]. Briefly, *C. sakazakii* was activated in sterilized LB broth for 24 h at 37 $^{\circ}\text{C}$ with a rotation speed of 100 rpm. The activated strains (5 μL) were inoculated in LB broth and cultivated for 12 h at 37 $^{\circ}\text{C}$ with a rotation speed of 100 rpm. The solution was then diluted with sterilized 0.9% NaCl to different concentration gradients, and 50 μL of each bacterial solution with various concentrations was inoculated on a solid medium for spreading plates. After 12 h of cultivation at 37 $^{\circ}\text{C}$, the bacterial solution concentration was determined by counting. Second, total DNA in *C. sakazakii* was extracted using Bacterial Genomic DNA Rapid Extraction Kit. The original bacterial solution (1 mL) was centrifuged at 10,000 rpm for 5 min at 4 $^{\circ}\text{C}$. The precipitate was collected and added to a sterile 0.9% NaCl aqueous solution (500 μL). The precipitate was well dispersed in the mixture by vortex mixing. The mixture was centrifuged at 10,000 rpm for 5 min to collect the precipitate. Afterwards, 200 μL of DNA extraction solution was added to the precipitate, followed by vigorous vortexing. It was then heated at 100 $^{\circ}\text{C}$ for 10 min and followed by rapid cooling in the refrigerator for another 10 min. The mixture was centrifuged at 10,000 rpm for 3 min, and the supernatant was collected and stored at 4 $^{\circ}\text{C}$.

The DNA extraction samples of *C. sakazakii*-contaminated infant formula powder were prepared according to Zhao's method [34]. Three actual samples were prepared by adding cultured *C. sakazakii* (5.4×10^1 , 5.4×10^2 , and 5.4×10^3 CFU mL⁻¹) into infant formula powder (1.0 g) which was dissolved in buffer peptone water (10.0 mL). The solution was thoroughly mixed, followed by removing proteins and fats using chloroform. Typically, after the addition of 1.0 mL chloroform, the contaminated suspension was kept shaking for 1 min. The resultant mixture was centrifuged at 3000 rpm for 5 min at room temperature. The supernatant was then collected and transferred into a centrifugal tube, followed by centrifugation at 12,000 rpm for another 5 min. The precipitation was then collected and used for total DNA extraction according to the previous procedures. The prepared real samples were stored at 4 °C in a refrigerator for direct electrochemical detection and PCR.

The PCR amplification was carried out in a reaction system containing 25.0 µL of 2 × Taq PCR Mix, 5.0 µL of total DNA extraction with different concentrations as the template DNA, 1.0 µL of 10.0 µM Primer F, 1.0 µL of 10.0 µM Primer R, and 18.0 µL of double distilled H₂O. The PCR amplification procedures were as follows: pre-denaturation at 95 °C for 5 min, 30 amplification cycles (denaturation at 95 °C for 30 s, annealing at 58 °C for 40 s, and extension at 72 °C for 40 s), and finally, extension at 72 °C for 5 min. The obtained PCR product was stored at 4 °C in the refrigerator. Agarose gel electrophoresis was used to verify the PCR products. The measurement was performed on a 1% agarose gel at 120 V for 40 min in 1 × TAE buffer, and the electrophoresis bands were observed under ultraviolet light.

2.7. Electrochemical Measurement

Cyclic voltammetry (CV) was used to characterize the catalytic ability of Cu-MOF and AuNPs@Cu-MOF to glucose. The experiments were performed in phosphate buffer solution (PBS, 0.1 M, pH 7.0) containing 5.0 mM glucose within a potential window of −0.8~0.4 V at a scan rate of 50 mV s⁻¹.

CV and electrochemical impedance spectroscopy (EIS) were adopted for monitoring the fabrication process of GCE. The CV experiments were carried out in 0.1 M KCl containing 5.0 mM [Fe(CN)₆]^{3-/4-} between the potential window −0.5 V and 0.6 V with a scan rate of 50 mV s⁻¹. The EIS measurements were performed in 0.1 M KCl containing 5.0 mM [Fe(CN)₆]^{3-/4-} in a frequency range of 0.1~100 kHz.

The analytical performance of our constructed biosensor was evaluated by differential pulse voltammetry (DPV). As shown in Figure 1, the fabricated *ompA* biosensor (BSA-blocked cDNA/Au/GCE) was incubated in hybridized buffer containing various concentrations of the *ompA* target. The hybridization reaction was carried out at 37 °C for 60 min. After rinsed with Tris-HCl solution (10 mmol L⁻¹, pH 7.4), the obtained tDNA/cDNA/Au/GCE was incubated in sDNA-AuNPs@Cu-MOF for 90 min at 37 °C to undergo the hybridization reaction between tDNA and sDNA. The resultant modified electrode also rinsed with Tris-HCl solution (10 mmol L⁻¹, pH 7.4) was named as sDNA-Au@Cu-MOF/tDNA/cDNA/Au/GCE. The DPV measurements were performed in a potential range from −0.5 to 0.4 V in 0.1 mol L⁻¹ phosphate buffer solution (pH = 7.0) containing 6.0 mM glucose. The DPV parameters were set as follows: a pulse amplitude of 50 mV and a pulse width of 0.05 s.

3. Results and Discussion

3.1. Characteristics of Cu-MOF and AuNPs@Cu-MOF

The morphology of Cu-MOF and AuNPs@Cu-MOF was characterized by SEM, and the images are shown in Figure 2. As shown in Figure 2A,B, the particle size of Cu-MOF ranges from 150 to 500 nm. The particles appear as cup-like structures. Compared with Cu-MOF, after the immobilization of chemically reduced AuNPs, the surface of AuNPs@Cu-MOF (Figure 2C,D) becomes rougher. This indicates the successful loading of AuNPs on Cu-MOF. Moreover, the particle size of AuNPs@Cu-MOF also ranges from 150 to 500 nm, and the shape of AuNPs@Cu-MOF is still in a cup-like structure. More importantly, from

the SEM images of Cu-MOF and AuNPs@Cu-MOF, the background is clear, demonstrating the stable structure possessed by these materials.

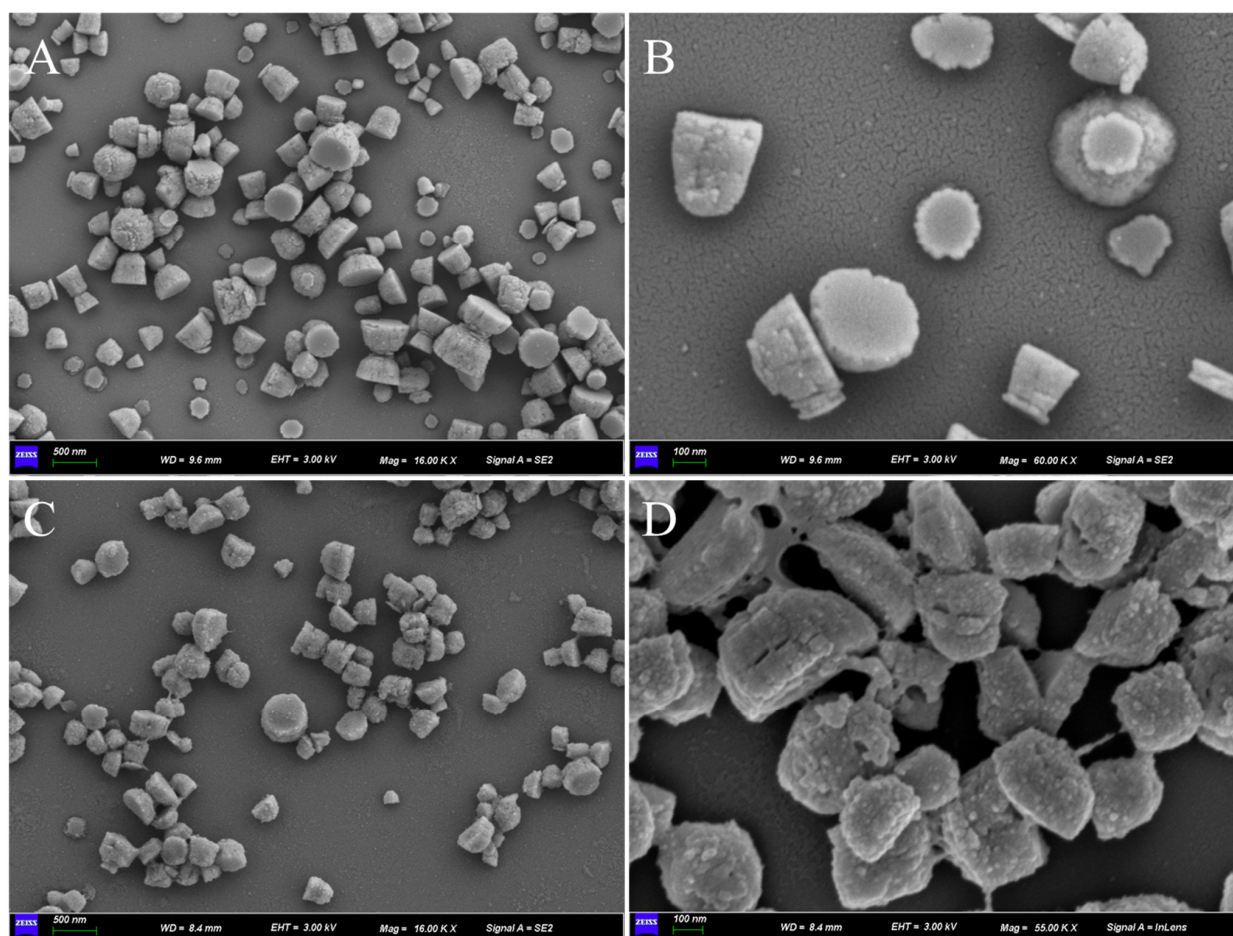


Figure 2. SEM images of Cu-MOF and AuNPs@Cu-MOF obtained with different magnifications. Cu-MOF: (A) and (B) and AuNPs@Cu-MOF: (C) and (D).

The elemental composition of Cu-MOF and AuNPs@Cu-MOF was characterized by using XPS. As displayed in Figure 3A, the survey spectrum of Cu-MOF gives the main peaks located at 934.2, 532.1, 400.0, and 285.3 eV that are ascribed to Cu2p [32], O1s [37], N1s [37], and C1s [37], respectively. The Cu2p spectrum in Cu-MOF (Figure 3B) shows that the binding energies of Cu²⁺ 2p_{1/2} and Cu²⁺ 2p_{3/2} are about 954.1 and 934.1 eV, respectively. From the XPS survey of AuNPs@Cu-MOF (Figure 3C), apart from the peaks of Cu2p, O1s, N1s, and C1s, a new peak at 87.7 eV can be found. This peak is assigned to Au4f [14]. In addition, the binding energies of Cu²⁺ 2p_{1/2} and Cu²⁺ 2p_{3/2} of the Cu2p spectrum in AuNPs@Cu-MOF (Figure 3D) are about 954.9 and 934.9 eV, respectively. The immersed peak of Au4f in the AuNPs@Cu-MOF XPS survey indicates the loading of AuNPs on Cu-MOF, which is in accordance with the result obtained from SEM characterization. Compared with the binding energy of Cu²⁺ 2p_{1/2} and 2p_{3/2} in Cu-MOF, the positive shift of Cu²⁺ 2p_{1/2} and 2p_{3/2} in AuNPs@Cu-MOF shows that the electron was away from divalent Cu in the structure of AuNPs@Cu-MOF. This may cause the valence of Cu in AuNPs@Cu-MOF to be higher than that in Cu-MOF. Moreover, no peaks attributed to Cu⁰ and Cu⁺ in Cu-MOF and AuNPs@Cu-MOF were observed. This indicates that Cu-MOF was formed through the reaction between Cu²⁺ and organic ligands, and no structural damage of Cu-MOF occurred during the reduction of AuCl⁴⁻ to Au⁰ using NaBH₄ as a reducing agent.

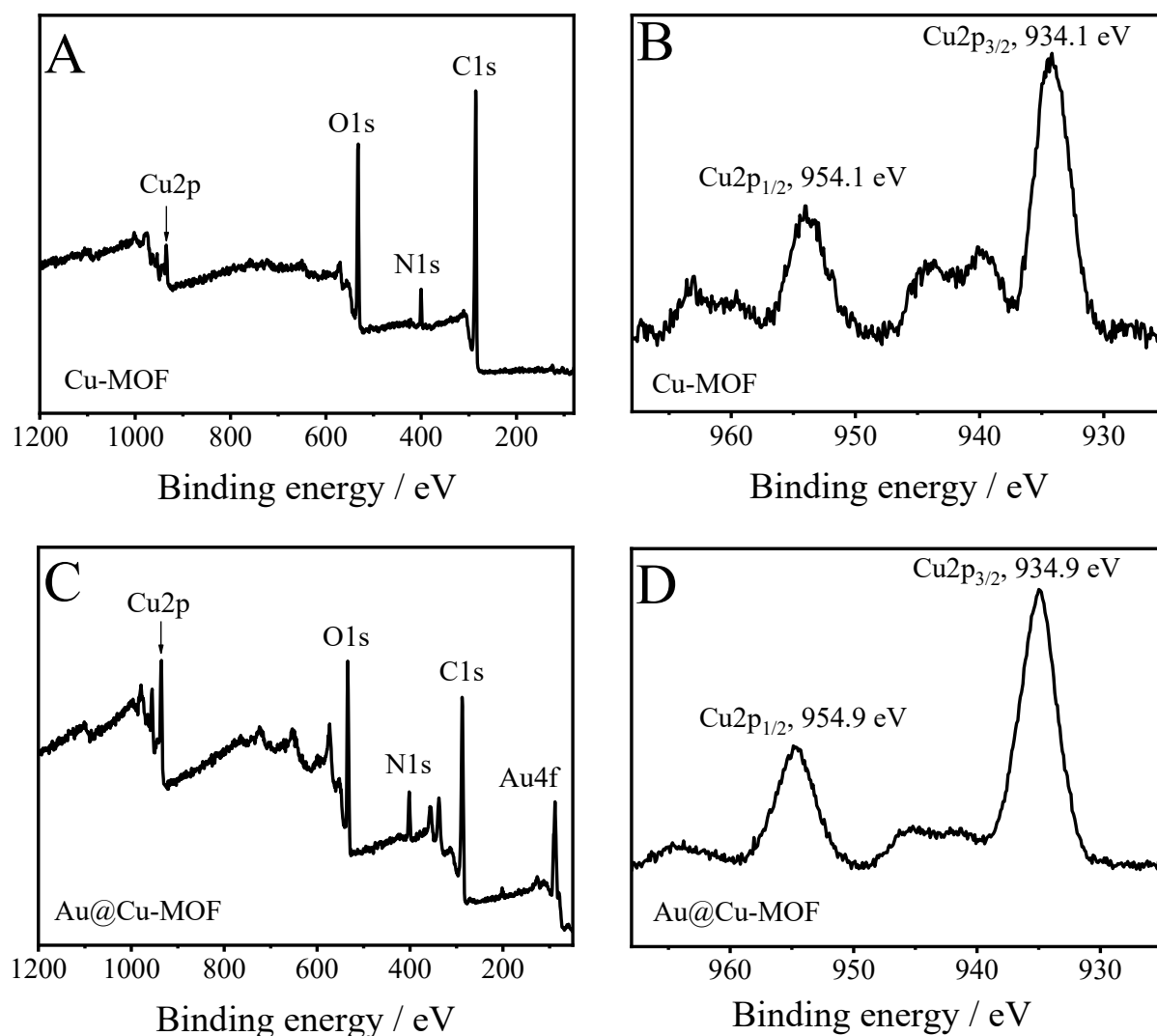


Figure 3. (A) XPS survey spectrum of Cu-MOF, (B) Cu2p region in Cu-MOF, (C) XPS survey spectrum of AuNPs@Cu-MOF, and (D) Cu2p region in AuNPs@Cu-MOF.

The mimetic glucose oxidase activity of Cu-MOF and AuNPs@Cu-MOF was investigated and compared by CV and DPV. Figure 4A shows the CV curves obtained on different electrodes in 0.1 M pH 7.0 PBS with or without 5 mM glucose. As shown in the figure, no redox peaks were observed within the sweeping potential window of $-0.8\sim 0.4$ V in the presence (curve b) or absence (curve a) of 5 mM glucose. In the absence of glucose, an oxidation peak was recorded at about -0.11 V and a reduction peak at about -0.22 V on Cu-MOF/GCE and AuNPs@Cu-MOF/GCE. In the presence of 5 mM glucose, however, the redox peak currents at -0.11 V and -0.22 V were dramatically increased. Furthermore, the peak current values of oxidation and reduction peaks were higher at AuNPs@Cu-MOF/GCE than those at Cu-MOF/GCE. The electrocatalytic ability of Cu-MOF and AuNPs@Cu-MOF to glucose was also evaluated and compared by DPV (Figure 4B) in a potential range between -0.8 and 0.4 V. As can be seen from the figure, the absolute values of peak current on AuNPs@Cu-MOF/GCE and Cu-MOF/GCE were calculated to be 34.601 (ΔI_2) and 27.706 μA (ΔI_1), respectively. The electrochemical reaction that occurred on the modified electrode may follow the reaction steps given below:



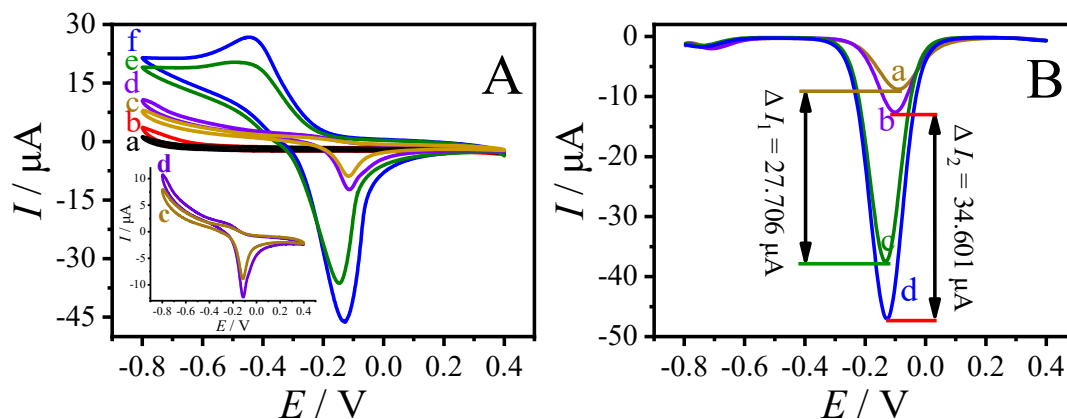


Figure 4. (A) CV curves obtained on different electrodes in 0.1 M pH 7.0 PBS with (b, e, and f) or without (a, c, and d) 5 mM glucose at a scan rate of 50 mV s^{-1} . (a) and (b) were at bare GCE, (c) and (e) were at Cu-MOF/GCE, and (d) and (f) were at AuNPs@Cu-MOF/GCE. (B) DPV curves obtained at Cu-MOF/GCE (a and c) and AuNPs@Cu-MOF/GCE (b and d) in 0.1 M pH 7.0 PBS with (c and d) or without (a and b) 5 mM glucose.

It can be inferred from the above reaction mechanism that the amplified signal on Cu-MOF/GCE and AuNPs@Cu-MOF/GCE is due to the electrocatalytic ability of Cu(II) anchored in MOFs to glucose [38,39]. The enhanced catalytic ability of AuNPs@Cu-MOF may result from the synergistic effect of AuNPs and Cu-MOF [25]. It is worth mentioning that the higher valence of Cu in AuNPs@Cu-MOF than that in Cu-MOF may also be the reason for its enhanced oxidation ability to glucose.

3.2. Electrochemical Characterization of Biosensor Fabrication

The step-by-step assembly of the biosensor was characterized by CV and EIS in 0.1 M KCl containing 5.0 mM $[\text{Fe}(\text{CN})_6]^{3-/4-}$. As exhibited in Figure 5A, a pair of well-defined redox peaks were observed on bare GCE and different modified GCEs. The absolute values of the redox peaks recorded on Au/GCE (Figure 5A, curve b) were increased compared with those recorded on bare GCE (Figure 5A, curve a), indicating the electron facilitation of the electrodeposited AuNPs. Afterwards, the absolute values of the redox peak currents decreased step by step with the immobilization of cDNA (Figure 5A, curve c), BSA (Figure 5A, curve d), tDNA (Figure 5A, curve e), and sDNA-AuNPs@Cu-MOF (Figure 5A, curve f) on Au/GCE, indicating the inhibited diffusion of $[\text{Fe}(\text{CN})_6]^{3-/4-}$ redox probe. In addition, the variation trend of charge transfer resistance (R_{ct}) of GCE and different modified GCEs analyzed by EIS (Figure 5B) was in accordance with the CV result. As is clearly shown in Fig. 5B, bare GCE showed a small semicircle with an R_{ct} of 217.7 Ω (Figure 5B, curve a). The obtained R_{ct} on Au/GCE was significantly decreased to 127.3 Ω (Figure 5B, curve b), owing to fast electron transfer on Au/GCE. After stepwise modification of cDNA (Figure 5B, curve c), BSA (Figure 5B, curve d), tDNA (Figure 5B, curve e), and sDNA-AuNPs@Cu-MOF (Figure 5B, curve f) on Au/GCE, the R_{ct} increased step by step to 446.3, 600.6, 1075.0, and 1398.0 Ω . This demonstrates the inhibited diffusion of $[\text{Fe}(\text{CN})_6]^{3-/4-}$ redox probe in 0.1 M KCl solution. Both the CV and EIS characterizations show the successful fabrication of the *ompA* gene-sensor and its ability to bind target probe and signal probe via DNA hybridization.

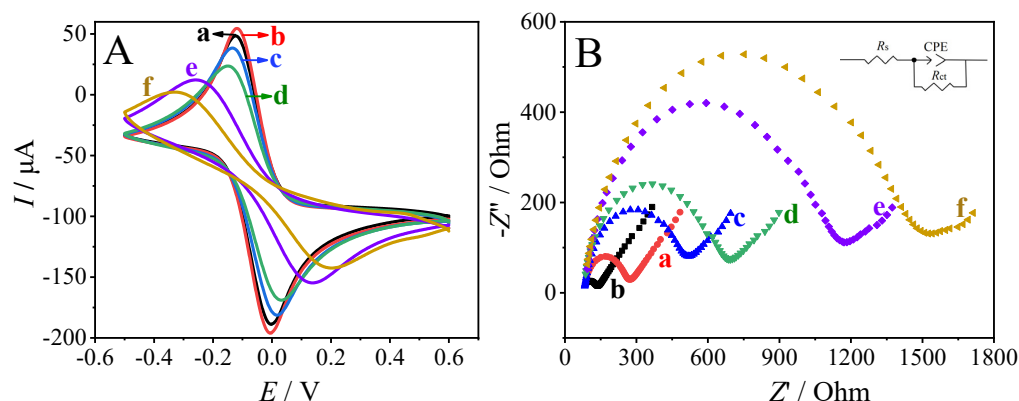


Figure 5. CVs (A) and EIS plots (B) recorded on bare GCE (a), Au/GCE (b), cDNA/Au/GCE (c), BSA blocked cDNA/Au/GCE (d), tDNA/BSA/cDNA/Au/GCE (e), and sDNA-AuNPs@Cu-MOF/tDNA/cDNA/Au/GCE (f) in 0.1 M KCl containing 5 mM $[\text{Fe}(\text{CN})_6]^{3-/4-}$.

3.3. Analytical Performance of the Biosensor

The analytical performance of the biosensor for detecting the *ompA* gene was investigated by using the DPV method. Before conducting DPV measurements, a number of factors, including the hybridization time between cDNA and tDNA, hybridization time between tDNA and sDNA, the concentration of AuNPs@Cu-MOF, and the concentration of glucose in the electrochemical detection buffer, were optimized. The relationship between the change of peak current (ΔI , $\Delta I = I_0 - I_1$, where I_0 and I_1 were the current responses of the biosensor to 0 and 10 nmol L⁻¹ tDNA, respectively) and different parameters was shown in Figure 6. As displayed in the figure, it is easy to conclude that the optimal conditions for detecting the *ompA* gene were 90 min for cDNA and tDNA hybridization, 90 min for tDNA and sDNA hybridization, 1.5 mg mL⁻¹ of AuNPs@Cu-MOF, and 6 mM glucose in electrochemical detection buffer.

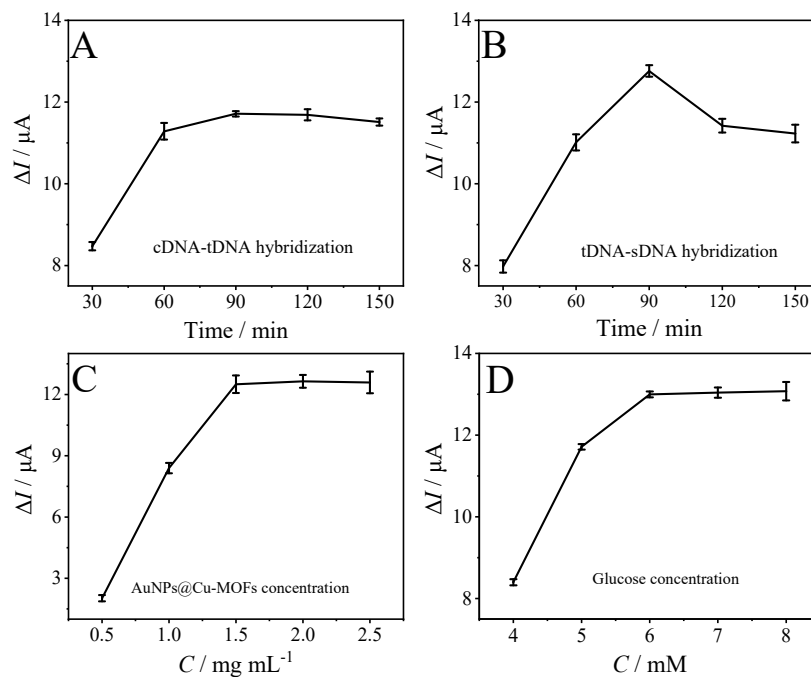


Figure 6. Parameter optimization of the biosensor. (A) Effect of cDNA and tDNA hybridization time, (B) effect of tDNA and sDNA hybridization time, (C) effect of Au@Cu-MOF concentration, and (D) effect of glucose concentration. The concentration of tDNA was 10 nM.

The biosensor was then applied in the detection target *ompA* gene under optimal conditions, and the DPV responses to various concentrations of *ompA* are displayed in Figure 7A. As clearly shown in the figure, the DPV response increases with the increasing *ompA* concentration. In this biosensing system, cDNA, tDNA, and sDNA-AuNPs@Cu-MOF can form a sandwich-typed structure of cDNA-tDNA-sDNA-AuNPs@Cu-MOF. As a result, with the increasing concentration of tDNA, more sDNA-AuNPs@Cu-MOF can react with tDNA, leading to the increased electrocatalytic signal of glucose. The DPV response of ΔI exhibited a linear relationship with the logarithm tDNA concentration in a range of $1 \text{ fmol L}^{-1} \sim 10 \text{ nmol L}^{-1}$ (Figure 7B). The linear regression equation was written as $\Delta I (\mu\text{A}) = 1.749 \lg C (\text{mol} \cdot \text{L}^{-1}) + 27.01$ ($R = 0.997$, Equation (1)) with a detection limit of (LOD) 0.42 fmol L^{-1} ($S/N = 3$).

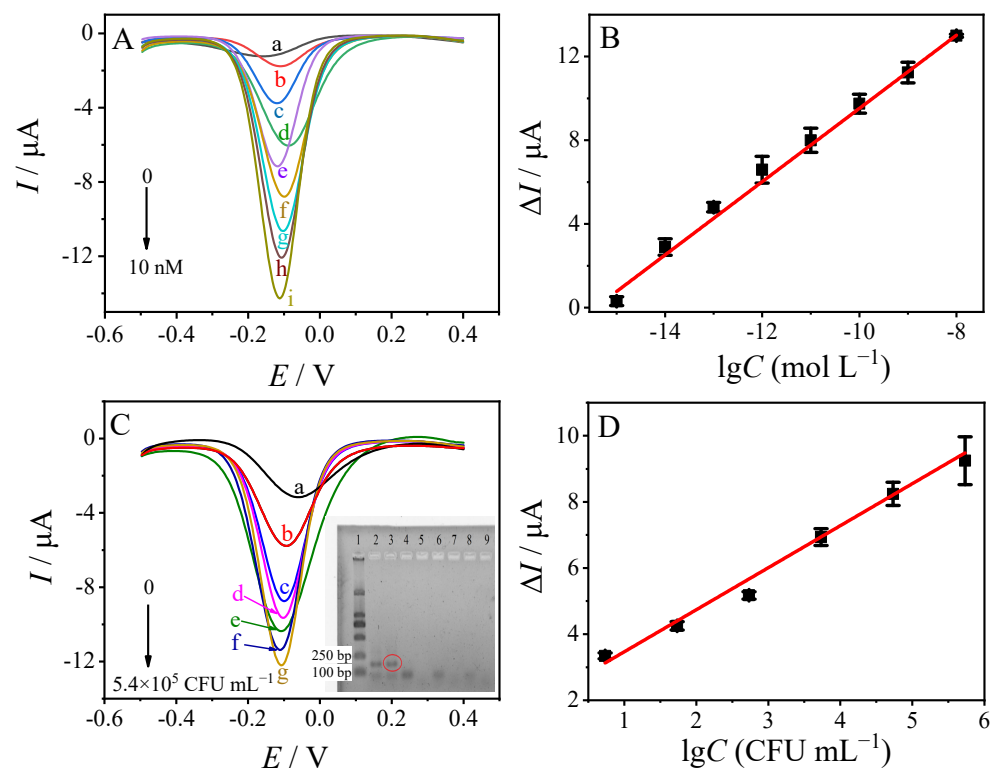


Figure 7. (A) DPV responses of the biosensor to different tDNA concentrations in 0.1 M pH 7.0 PBS contained 6.0 mM glucose. From top to bottom: (a) 0 M, (b) 1 fM, (c) 10 fM, (d) 100 fM, (e) 1 pM, (f) 10 pM, (g) 100 pM, (h) 1 nM, and (i) 10 nM. Inset: (B) The calibration curve of ΔI vs. the logarithm of tDNA in the range of 1 fM~10 nM. (C) The DPV responses of the biosensor towards various concentrations of *ompA* gene segments in total DNA extracted from different concentrations of *Cronobacter sakazakii*. From top to bottom are the curves of detecting 0, 5.4, 54, 5.4×10^2 , 5.4×10^3 , 5.4×10^4 , 5.4×10^5 CFU mL⁻¹. Inset: agarose gel electrophoresis for marker (lane 1), *ompA* gene PCR products of 5.4×10^5 , 5.4×10^4 , 5.4×10^3 , 5.4×10^2 , 54, and 5.4 CFU mL⁻¹ (from lanes 2 to 7, respectively). (D) The linear relationship between ΔI and the logarithm concentration of *Cronobacter sakazakii*.

3.4. Detection of *ompA* Gene Segments Extracted from *Cronobacter sakazakii*

The analytical performance of the fabricated biosensor was also investigated and evaluated by using it to directly detect *ompA* gene segments in total DNA extracted from *C. sakazakii*. The *ompA* gene segments extracted from *C. sakazakii* were amplified with PCR, and the products were confirmed with agarose gel electrophoresis (Figure 7C, inset). In this figure, lanes 2 to 7 were the PCR products of various concentrations of *C. sakazakii* (5.4×10^5 , 5.4×10^4 , 5.4×10^3 , 5.4×10^2 , 54, and 5.4 CFU mL⁻¹, respectively). Compared with the marker (lane 1), the band at between 100 bp and 250 bp in lanes 2 and 3 is related

to PCR products of *ompA* gene segments. The DPV responses on the biosensor for *ompA* segments in total DNA extracted from various concentrations of *C. sakazakii* are shown in Figure 7C. As shown in the figure, the recorded DPV response on the biosensor varied with the varying concentration of *C. sakazakii*. It is obvious that the DPV response increased with the increasing concentration of *C. sakazakii*. A good linear relationship between ΔI and the logarithm of the *C. sakazakii* concentration was obtained in a range of $5.4\text{--}5.4 \times 10^5$ CFU mL⁻¹ with an equation of ΔI (μA) = $1.271 \lg C$ (CFU mL⁻¹) + 2.196 ($R = 0.996$, Equation (2)). The LOD was calculated to be 0.35 CFU mL⁻¹ ($S/N = 3$).

The analytical performance of the fabricated biosensor was compared with other reported biosensors for the detection of *C. sakazakii*, and the results are listed in Table 2. As shown in the table, the detection linear range of *C. sakazakii* of our biosensor is broader than most of the electrochemical listed biosensors [12–16], and LOD is the lowest among these biosensors.

Table 2. Comparison of the different detection methods.

Materials/ Nanomaterials	Analytical Method	Linear Range (CFU mL ⁻¹)	Detection Limit (CFU mL ⁻¹)	Refs.
AuNPs	colorimetric	$7.1 \times 10^3 \sim 7.1 \times 10^7$	-	[12]
G-rich DNA probes formed DNAzyme	colorimetric	$2 \sim 1.2 \times 10^3$	1.2	[13]
BQDs-AuNPs	i-t	$7.8 \times 10^0 \sim 7.8 \times 10^6$	2.6	[14]
MB-anchored GO	DPV	$1.0 \times 10^2 \sim 1.0 \times 10^7$	73	[15]
G-quadruplex DNAzyme	i-t	$3.84 \times 10^4 \sim 2.4 \times 10^7$	501	[16]
Au@Cu-MOF	DPV	$5.4 \times 10^0 \sim 5.4 \times 10^5$	0.35	This work

3.5. Selectivity, Reproducibility, and Stability of Biosensors

The specificity of the fabricated biosensor was evaluated with the DPV method by using the biosensor in detecting various DNA sequences. These sequences were tDNA (10 pmol L⁻¹), noncomplementary DNA (NC, 100 pmol L⁻¹), single-base mismatched DNA (Mis-1, 100 pmol L⁻¹), double-base mismatched DNA (Mis-2, 100 pmol L⁻¹), three-base mismatched DNA (Mis-3, 100 pmol L⁻¹), and DNA extracts from *Escherichia coli* (*E. coli*, 1.0×10^3 CFU mL⁻¹) and *Salmonella* (1.0×10^3 CFU mL⁻¹). The DPV responses to these sequences are shown in histogram style in Figure 8A. The fabricated biosensor gave a strong response to tDNA in the detection buffer and tDNA mixed with other DNA sequences (Figure 8A, column Mixture). The calculated ΔI to tDNA and tDNA in the mixture were $7.996 \pm 0.580 \mu\text{A}$ and $8.483 \pm 0.871 \mu\text{A}$, respectively. This shows that the difference in DPV response on the biosensor for tDNA and tDNA in a mixture was little. Compared to the tDNA signal, the DPV response decreased dramatically to other DNA sequences and DNA extracts from *E. coli* and *Salmonella*. These results indicate that the fabricated biosensor has good selectivity for target *ompA*.

The fabrication reproducibility of the electrochemical DNA sensor was also investigated before the application in the detection of *ompA* gene segments in real samples. Five GCEs were used to fabricate five biosensors for the detection of a 10 pM target, and ΔI obtained on each biosensor is shown in Figure 8B. A relative standard deviation of 4.81% was obtained within these five constructed biosensors, showing good reproducibility of the biosensor. The storage stability of the fabricated biosensor was also investigated (Figure 8C). After 3, 7, and 14 days of storage, the obtained ΔI were 97.2%, 91.8%, and 86.7% of the initial signal (0 day). This suggests that the biosensor has satisfactory storage stability.

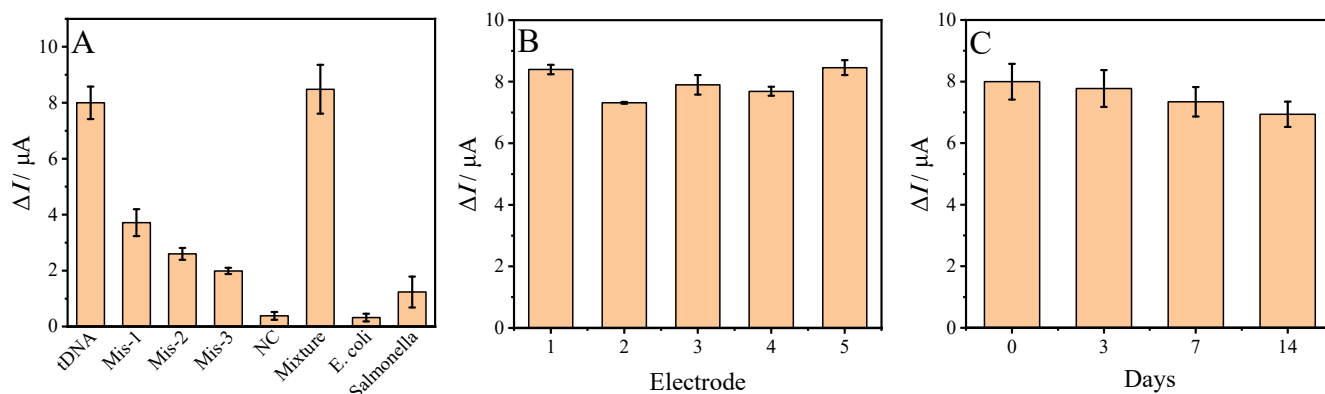


Figure 8. (A) Selectivity of the biosensor toward different DNA sequences, (B) fabrication reproducibility of the biosensor, and (C) storage stability of the biosensor.

3.6. Application in Direct Detection of *C. sakazakii* in Real Samples

Finally, the biosensor was applied in the detection of *C. sakazakii* in real samples. Three pretreated samples of infant formula contaminated with different concentrations (5.4×10^1 , 5.4×10^2 , and 5.4×10^3 CFU mL⁻¹) of *C. sakazakii*. The biosensor was then used for the detection of *ompA* gene segments in total DNA extracts. The detected concentrations of these samples were calculated according to Equation (2), and the results are listed in Table 3. As shown in the table, the recovery of these samples ranged from $87.5\% \pm 7.6\%$ to $107.3\% \pm 3.7\%$, which shows that the constructed sensor has applicability in the detection of the *ompA* gene in real samples.

Table 3. Detection of *C. sakazakii* in real samples ($N = 3$).

Sample	Add (CFU mL ⁻¹)	Found (CFU mL ⁻¹)	Recovery (%)
1	5.4×10^1	57.9 ± 2.1	107.3 ± 3.7
2	5.4×10^2	572.4 ± 54.8	105.9 ± 9.5
3	5.4×10^3	4824.7 ± 584	87.5 ± 7.6

4. Conclusions

In this research work, we designed an electrochemical DNA sensor for the selective detection of the *ompA* gene of *C. sakazakii* by exploiting the excellent electrocatalytic activity of AuNPs@Cu-MOF to glucose. The biosensor showed good linearity from 1 fmol L⁻¹ to 10 nmol L⁻¹ to target the *ompA* gene with a LOD of 0.42 fmol L⁻¹. In addition, the biosensor can be used for direct detection of *ompA* gene fragments in total DNA extracts from *C. sakazakii* with a LOD as low as 0.35 CFU mL⁻¹. The constructed electrochemical biosensor possessed good selectivity, fabrication reproducibility and storage stability, which can be applied in the detection of the *ompA* gene in actual samples with good credibility.

Author Contributions: Conceptualization, X.C. and Y.Y.; methodology, X.C. and Y.Y.; validation, X.C. and Y.Y.; formal analysis, H.Z., X.C. and Y.Y.; investigation; H.Z., G.X., Y.C., X.L., S.W., F.J., P.Z. and C.L.; resources, X.C., Y.Y. and Y.T.; data curation, H.Z. and X.C.; writing—original draft preparation, H.Z., X.C. and Y.Y.; writing—review and editing, X.C., Y.Y. and Y.T.; visualization, H.Z., X.C. and Y.Y.; supervision, X.C. and Y.Y.; project administration, X.C. and Y.Y.; funding acquisition, X.C., Y.Y. and Y.T. All authors have read and agreed to the published version of the manuscript.

Funding: This research was funded by Anhui Province’s Major Science and Technology Special Projects, grant numbers 202103a07020003 and 202003a06020018; Anhui Provincial Key R&D Programmes, grant numbers 202024a07020038 and 202104a06020005; and Innovation and Entrepreneurship Training Program for Undergraduate of Hefei University of Technology: X202210359867.

Institutional Review Board Statement: Not applicable.

Informed Consent Statement: Not applicable.

Data Availability Statement: Not applicable.

Acknowledgments: The authors thank the Technology Center of Hefei Customs District for providing the strains.

Conflicts of Interest: The authors declare no conflict of interest. The funders had no role in the design of the study; in the collection, analyses, or interpretation of data; in the writing of the manuscript; or in the decision to publish the results.

References

1. Parra-Flores, J.; Maury-Sintjago, E.; Rodriguez-Fernández, A.; Acuña, S.; Cerda, F.; Aguirre, J.; Holy, O. Microbiological Quality of Powdered Infant Formula in Latin America. *J. Food Prot.* **2020**, *83*, 534–541. [[CrossRef](#)] [[PubMed](#)]
2. Yin, M.; Wang, Z.; Xie, P.; Han, L.; Li, L.; Wang, H.; Qiao, X.; Deng, Q. Fluorescence sensing platform for *Cronobacter sakazakii* based on the cationic metal-organic frameworks modified upconversion nanoparticles. *Food Control.* **2023**, *145*, 109443. [[CrossRef](#)]
3. Yi, M.; He, P.; Li, J.; Zhang, J.; Lin, L.; Wang, L.; Zhao, L. A portable toolbox based on time-resolved fluoroimmunoassay and immunomagnetic separation for *Cronobacter sakazakii* on-site detection in dairy. *Int. Dairy J.* **2022**, *133*, 105425. [[CrossRef](#)]
4. Zhang, L.; Chen, Y.; Cheng, N.; Xu, Y.; Huang, K.; Luo, Y.; Wang, P.; Duan, D.; Xu, W. Ultrasensitive Detection of Viable *Enterobacter sakazakii* by a Continual Cascade Nanozyme Biosensor. *Anal. Chem.* **2017**, *89*, 10194–10200. [[CrossRef](#)] [[PubMed](#)]
5. Wu, Y.; Xiong, Y.; Chen, X.; Luo, D.; Gao, B.; Chen, J.; Huang, X.; Leng, Y.; Xiong, Y. Plasmonic ELISA based on DNA-directed gold nanoparticle growth for *Cronobacter* detection in powdered infant formula samples. *J. Dairy Sci.* **2019**, *102*, 10877–10886. [[CrossRef](#)]
6. Akineden, O.; Wittwer, T.; Geister, K.; Plötz, M.; Usleber, E. Nucleic acid lateral flow immunoassay (NALFIA) with integrated DNA probe degradation for the rapid detection of *Cronobacter sakazakii* and *Cronobacter malonaticus* in powdered infant formula. *Food Control.* **2019**, *109*, 106952.
7. Shukla, S.; Haldorai, Y.; Bajpai, V.K.; Rengaraj, A.; Hwang, S.K.; Song, X.; Kim, M.; Huh, Y.S.; Han, Y.-K. Electrochemical coupled immunosensing platform based on graphene oxide/gold nanocomposite for sensitive detection of *Cronobacter sakazakii* in powdered infant formula. *Biosens. Bioelectron.* **2018**, *109*, 139–149. [[CrossRef](#)]
8. Li, P.; Feng, X.; Chen, B.; Wang, X.; Liang, Z.; Wang, L. The Detection of Foodborne Pathogenic Bacteria in Seafood Using a Multiplex Polymerase Chain Reaction System. *Foods* **2022**, *11*, 3909. [[CrossRef](#)]
9. Xie, X.; Liu, Z. Simultaneous enumeration of *Cronobacter sakazakii* and *Staphylococcus aureus* in powdered infant foods through duplex TaqMan real-time PCR. *Int. Dairy J.* **2021**, *117*, 105019. [[CrossRef](#)]
10. Liu, J.; Xie, G.; Xiong, Q.; Mu, D.; Xu, H. A simple and sensitive aptasensor with rolling circle amplification for viable *Cronobacter sakazakii* detection in powdered infant formula. *J. Dairy Sci.* **2021**, *104*, 12365–12374. [[CrossRef](#)]
11. Liu, J.; Zhan, Z.; Liang, T.; Xie, G.; Aguilar, Z.P.; Xu, H. Dual-signal amplification strategy: Universal asymmetric tailing-PCR triggered rolling circle amplification assay for fluorescent detection of *Cronobacter* spp. in milk. *J. Dairy Sci.* **2020**, *103*, 3055–3065. [[CrossRef](#)]
12. Kim, H.S.; Kim, Y.J.; Chon, J.W.; Kim, D.H.; Yim, J.H.; Kim, H.; Seo, K.H. Two-stage label-free aptasensing platform for rapid detection of *Cronobacter sakazakii* in powdered infant formula. *Sens. Actuators B Chem.* **2017**, *239*, 94–99. [[CrossRef](#)]
13. Liu, Z.; Yuan, Y.; Wu, X.; Ning, Q.; Wu, S.; Fu, L. A turn-off colorimetric DNazyme-aptasensor for ultra-high sensitive detection of viable *Cronobacter sakazakii*. *Sens. Actuators B Chem.* **2020**, *322*, 128646. [[CrossRef](#)]
14. Cao, X.D.; Liu, M.L.; Lu, J.; Lv, H.G.; Han, J.Z.; He, S.D.; Ye, Y.K.; Chen, X.Y.; Wei, Z.J.; Zheng, H.S. An ultrasensitive biosensor for virulence *ompA* gene of *Cronobacter sakazakii* based on boron doped carbon quantum dots-AuNPs nanozyme and exonuclease III-assisted target-recycling strategy. *Food Chem.* **2022**, *391*, 133268. [[CrossRef](#)] [[PubMed](#)]
15. Peng, H.; Hui, Y.; Ren, R.; Wang, B.; Song, S.; He, Y.; Zhang, F. A sensitive electrochemical aptasensor based on MB-anchored GO for the rapid detection of *Cronobacter sakazakii*. *J. Solid State Electrochem.* **2019**, *23*, 3391–3398. [[CrossRef](#)]
16. Yuan, Y.Y.; Wu, X.Y.; Liu, Z.M.; Ning, Q.Q.; Fu, L.Q.; Wu, S.J. A signal cascade amplification strategy based on RT-PCR triggering of a G-quadruplex DNazyme for a novel electrochemical detection of viable *Cronobacter sakazakii*. *Analyst* **2020**, *145*, 4477–4483. [[CrossRef](#)]
17. Lv, M.; Zhou, W.; Tavakoli, H.; Bautista, C.; Xia, J.; Wang, Z.; Li, X. Aptamer-functionalized metal-organic frameworks (MOFs) for biosensing. *Biosens. Bioelectron.* **2020**, *176*, 112947. [[CrossRef](#)] [[PubMed](#)]
18. Lokhande, P.; Kulkarni, S.; Chakrabarti, S.; Pathan, H.; Sindhu, M.; Kumar, D.; Singh, J.; Kumar, A.; Mishra, Y.K.; Toncu, D.-C.; et al. The progress and roadmap of Metal-organic frameworks for high-performance supercapacitors. *Coord. Chem. Rev.* **2022**, *473*, 214771. [[CrossRef](#)]
19. Chuhadiya, S.; Himanshu; Suthar, D.; Patel, S.L.; Dhaka, M.S. Metal organic frameworks as hybrid porous materials for energy storage and conversion devices: A review. *Coord. Chem. Rev.* **2021**, *446*, 214115. [[CrossRef](#)]
20. Hou, R.; Miao, M.; Wang, Q.; Yue, T.; Liu, H.; Park, H.S.; Qi, K.; Xia, B.Y. Integrated Conductive Hybrid Architecture of Metal-organic Framework Nanowire Array on Polypyrrole Membrane for All-Solid-State Flexible Supercapacitors. *Adv. Energy Mater.* **2019**, *10*, 190189. [[CrossRef](#)]
21. Jia, T.; Gu, Y.; Li, F. Progress and potential of metal-organic frameworks (MOFs) for gas storage and separation: A review. *J. Environ. Chem. Eng.* **2022**, *10*, 108300. [[CrossRef](#)]

22. Coluccia, M.; Parisse, V.; Guglielmi, P.; Giannini, G.; Secci, D. Metal-organic frameworks (MOFs) as biomolecules drug delivery systems for anticancer purposes. *Eur. J. Med. Chem.* **2022**, *244*, 114801. [[CrossRef](#)]
23. Kajal, N.; Singh, V.; Gupta, R.; Gautam, S. Metal organic frameworks for electrochemical sensor applications: A review. *Environ. Res.* **2021**, *204*, 112320. [[CrossRef](#)] [[PubMed](#)]
24. Zhang, S.; Rong, F.; Guo, C.; Duan, F.; He, L.; Wang, M.; Zhang, Z.; Kang, M.; Du, M. Metal-organic frameworks (MOFs) based electrochemical biosensors for early cancer diagnosis in vitro. *Coord. Chem. Rev.* **2021**, *439*, 213948. [[CrossRef](#)]
25. Dang, W.; Sun, Y.; Jiao, H.; Xu, L.; Lin, M. AuNPs-NH₂/Cu-MOF modified glassy carbon electrode as enzyme-free electrochemical sensor detecting H₂O₂. *J. Electroanal. Chem.* **2020**, *856*, 113592. [[CrossRef](#)]
26. Wang, Z.; Huang, Y.; Xu, K.; Zhong, Y.; He, C.; Jiang, L.; Sun, J.; Rao, Z.; Zhu, J.; Huang, J.; et al. Natural oxidase-mimicking copper-organic frameworks for targeted identification of ascorbate in sensitive sweat sensing. *Nat. Commun.* **2023**, *14*, 1–9. [[CrossRef](#)]
27. Ling, Y.; Chu, Y.-R.; Gao, F.; Feng, Q.-Y.; Xie, H.-Q.; Shao, Y.; Wang, Q.-X. Immunoaffinity-Induced Signal Depression of Cu-MOF-74 for Label-Free Electrochemical Detection of Cardiac Troponin I. *J. Phys. Chem. C* **2022**, *126*, 9416–9424. [[CrossRef](#)]
28. Rezki, M.; Septiani, N.L.W.; Iqbal, M.; Harimurti, S.; Sambegoro, P.; Adhika, D.R.; Yulianto, B. Amine-functionalized Cu-MOF nanospheres towards label-free hepatitis B surface antigen electrochemical immunosensors. *J. Mater. Chem. B* **2021**, *9*, 5711–5721. [[CrossRef](#)]
29. Guo, X.; Lin, C.; Zhang, M.; Duan, X.; Dong, X.; Sun, D.; Pan, J.; You, T. 2D/3D Copper-Based Metal-Organic Frameworks for Electrochemical Detection of Hydrogen Peroxide. *Front. Chem.* **2021**, *9*, 743637. [[CrossRef](#)]
30. Zhang, D.; Zhang, J.; Zhang, R.; Shi, H.; Guo, Y.; Guo, X.; Li, S.; Yuan, B. 3D porous metal-organic framework as an efficient electrocatalyst for nonenzymatic sensing application. *Talanta* **2015**, *144*, 1176–1181. [[CrossRef](#)] [[PubMed](#)]
31. Sun, Y.M.; Li, Y.X.; Wang, N.; Xu, Q.Q.; Xu, L.; Lin, M. Copper-based Metal-organic Framework for Non-enzymatic Electrochemical Detection of Glucose. *Electroanalysis* **2018**, *30*, 474–478. [[CrossRef](#)]
32. Shen, W.-J.; Zhuo, Y.; Chai, Y.-Q.; Yuan, R. Cu-Based Metal-organic Frameworks as a Catalyst To Construct a Ratiometric Electrochemical Aptasensor for Sensitive Lipopolysaccharide Detection. *Anal. Chem.* **2015**, *87*, 11345–11352. [[CrossRef](#)] [[PubMed](#)]
33. Zhang, X.; Jiang, Y.; Zhu, M.; Xu, Y.; Guo, Z.; Shi, J.; Han, E.; Zou, X.; Wang, D. Electrochemical DNA sensor for inorganic mercury(II) ion at attomolar level in dairy product using Cu(II)-anchored metal-organic framework as mimetic catalyst. *Chem. Eng. J.* **2019**, *383*, 123182. [[CrossRef](#)]
34. Arikan, K.; Burhan, H.; Sahin, E.; Sen, F. A sensitive, fast, selective, and reusable enzyme-free glucose sensor based on monodisperse AuNi alloy nanoparticles on activated carbon support. *Chemosphere* **2022**, *291*, 132718. [[CrossRef](#)]
35. Soomro, R.A.; Akyuz, O.P.; Ozturk, R.; Ibupoto, Z.H. Highly sensitive non-enzymatic glucose sensing using gold nanocages as efficient electrode material. *Sens. Actuators B Chem.* **2016**, *233*, 230–236. [[CrossRef](#)]
36. Ye, Y.K.; Yan, W.W.; Liu, Y.Q.; He, S.D.; Cao, X.D.; Xu, X.; Zheng, H.S.; Gunasekaran, S. Electrochemical detection of Salmonella using an invA genosensor on polypyrrole-reduced graphene oxide modified glassy carbon electrode and AuNPs-horseradish peroxidase-streptavidin as nanotag. *Anal. Chem. Acta* **2019**, *1074*, 80–88. [[CrossRef](#)]
37. Wang, S.; Deng, W.; Yang, L.; Tan, Y.; Xie, Q.; Yao, S. Copper-Based Metal-Organic Framework Nanoparticles with Peroxidase-Like Activity for Sensitive Colorimetric Detection of Staphylococcus aureus. *ACS Appl. Mater. Interfaces* **2017**, *9*, 24440–24445. [[CrossRef](#)]
38. Wu, L.; Lu, Z.W.; Ye, J.S. Enzyme-free glucose sensor based on layer-by-layer electrodeposition of multilayer films of multi-walled carbon nanotubes and Cu-based metal framework modified glassy carbon electrode. *Biosens. Bioelectron.* **2019**, *135*, 45–49. [[CrossRef](#)]
39. Wang, X.; Ge, C.-Y.; Chen, K.; Zhang, Y.X. An ultrasensitive non-enzymatic glucose sensors based on controlled petal-like CuO nanostructure. *Electrochim. Acta* **2018**, *259*, 225–232. [[CrossRef](#)]

Disclaimer/Publisher’s Note: The statements, opinions and data contained in all publications are solely those of the individual author(s) and contributor(s) and not of MDPI and/or the editor(s). MDPI and/or the editor(s) disclaim responsibility for any injury to people or property resulting from any ideas, methods, instructions or products referred to in the content.